Supplementary Information (SI)

Divergent urbanization-induced impacts on global surface urban heat island trends since 1980s

Long Li, Wenfeng Zhan, Leiqiu Hu, Tirthankar Chakraborty, Zhihua Wang, Peng Fu, Dazhong Wang, Weilin Liao, Fan Huang, Huyan Fu, Jiufeng Li, Zihan Liu, Huilin Du, and Shasha Wang

This file includes:

A. Supplementary figures

Figures S1 to S12

B. Supplementary tables

Table S1

A. Supplementary figures

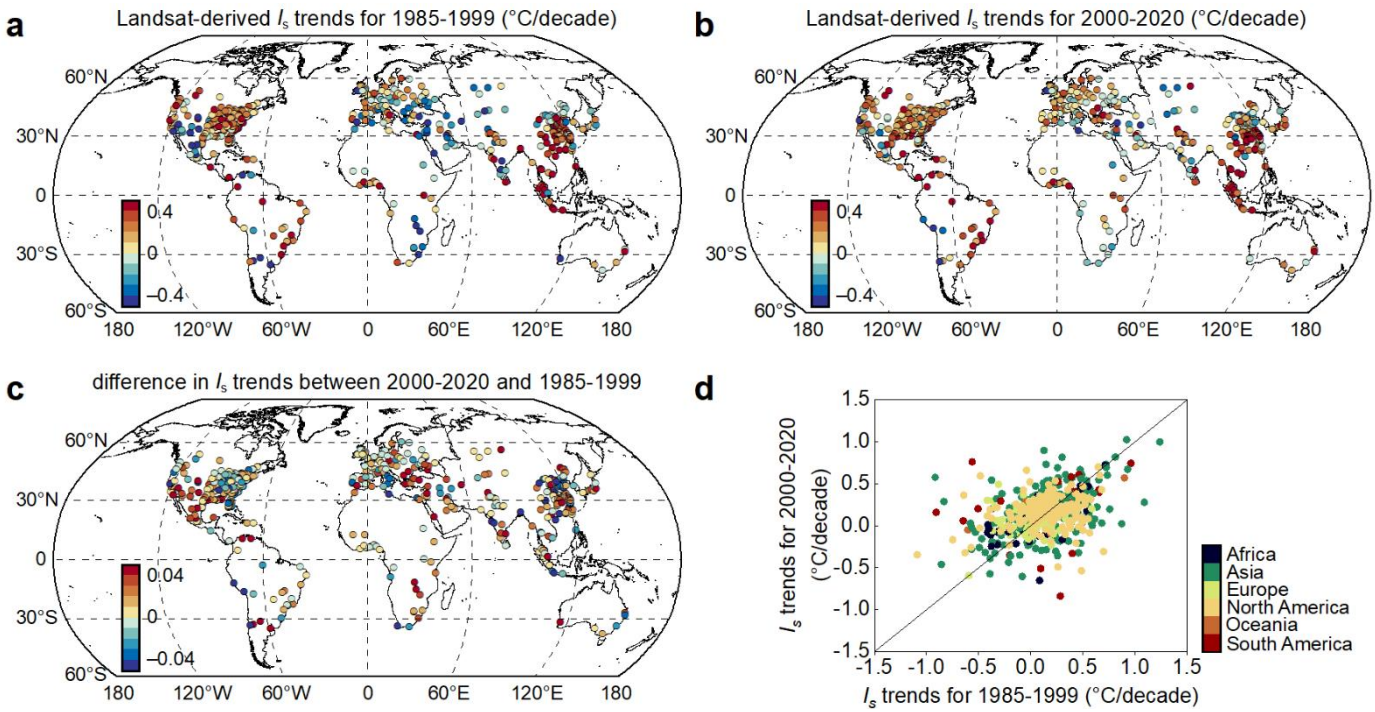

Figure S1. Comparison of surface urban heat island intensity (I_s) trends derived from reconstructed Landsat land surface temperature (LST) data across global major cities. The I_s trends (°C/decade) for the periods of 1985 – 1999 (**a**) and 2000 – 2020 (**b**), difference in I_s trends between these two periods (**c**), and the relationship of I_s trends between the two periods (**d**).

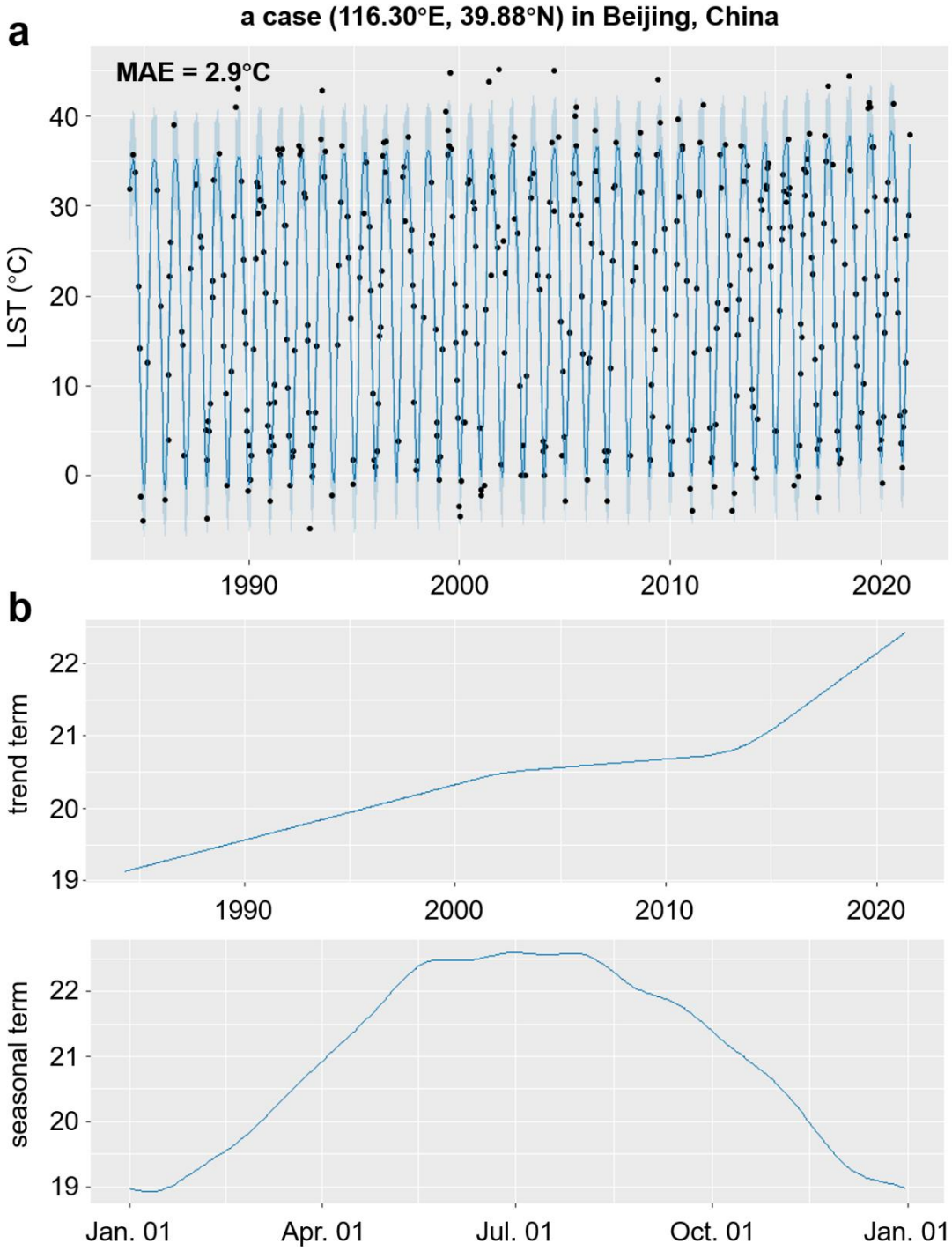

Figure S2. A case (116.30°E, 39.88°N) in Beijing, China to show the procedure of the Prophet model to reconstruct Landsat LST. Observed land surface temperature (LST, i.e., black dots) versus reconstructed LST curve (i.e., blue line) (**a**); the trend and seasonal terms obtained by using the Prophet model showing the interannual and seasonal variations of LST (**b**).

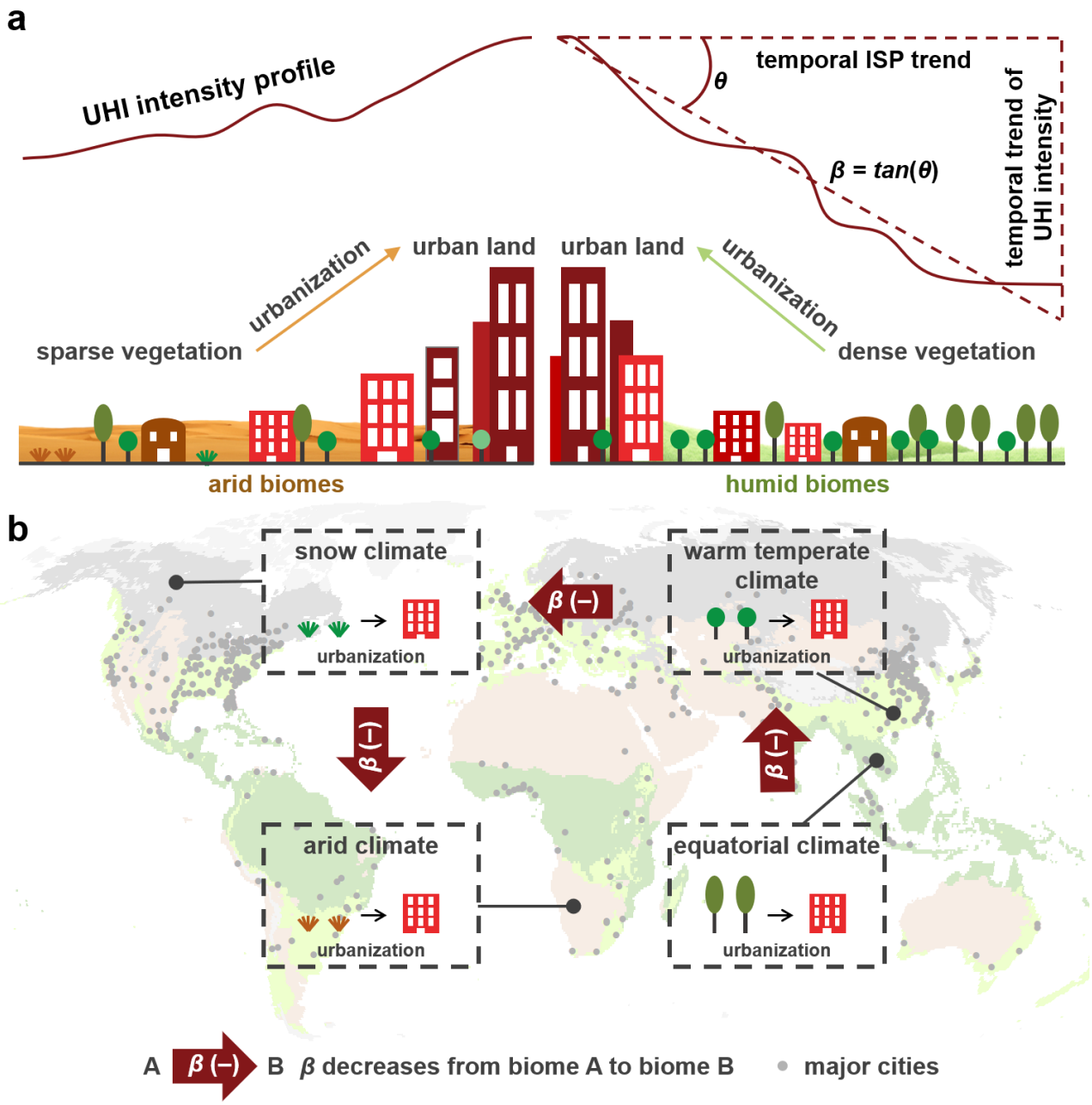

Figure S3. Conceptual diagram that displays the contrasts of urbanization-induced impacts on surface urban heat island intensity trends (β) across biome backgrounds. The conceptual illustration for the calculation of β (**a**), and the comparison of β across biome backgrounds (**b**). The β decreases gradually from equatorial to warm temperature, snow, and arid climates. The UHI and ISP are the abbreviations for urban heat island and impervious surface percentage, respectively.

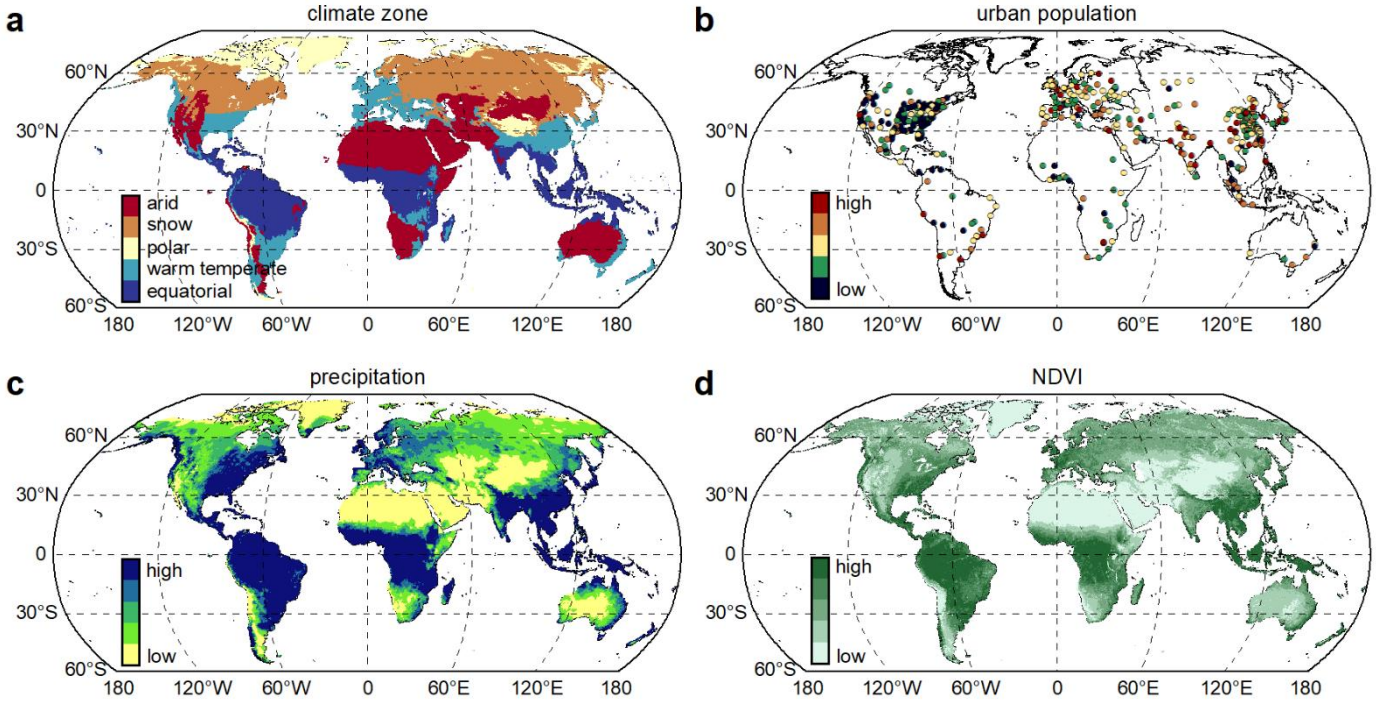

Figure S4. Spatial distribution of global major 511 cities as well as the corresponding climate zone, urban population, precipitation, and normalized difference vegetation index (NDVI). Climate zone (**a**), urban population (**b**), precipitation (**c**), and NDVI (**d**).

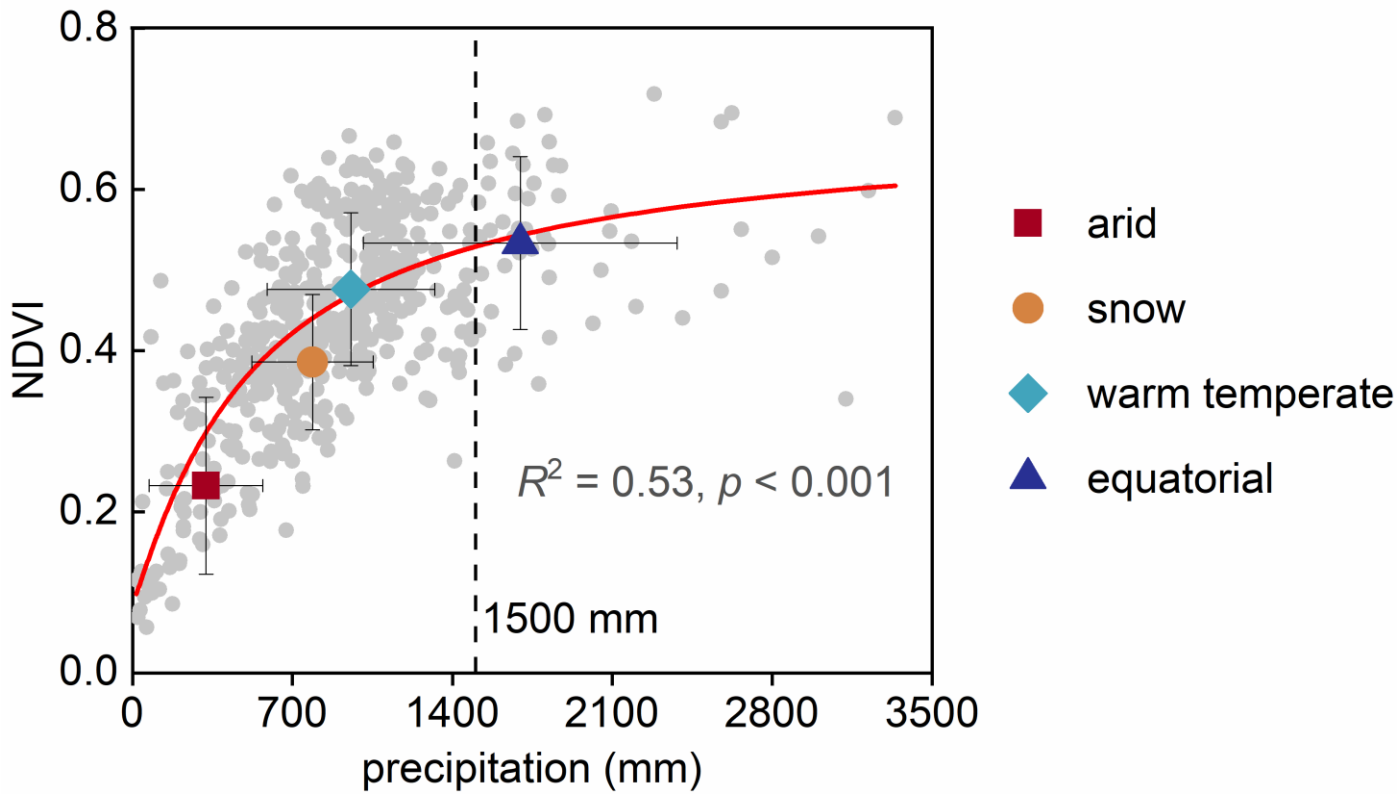

Figure S5. Relationship between rural NDVI and annual total precipitation across global cities. The rural NDVI generally increases with precipitation when precipitation is < 1500 mm, but there is no significant relationship between rural NDVI and precipitation when precipitation is > 1500 mm.

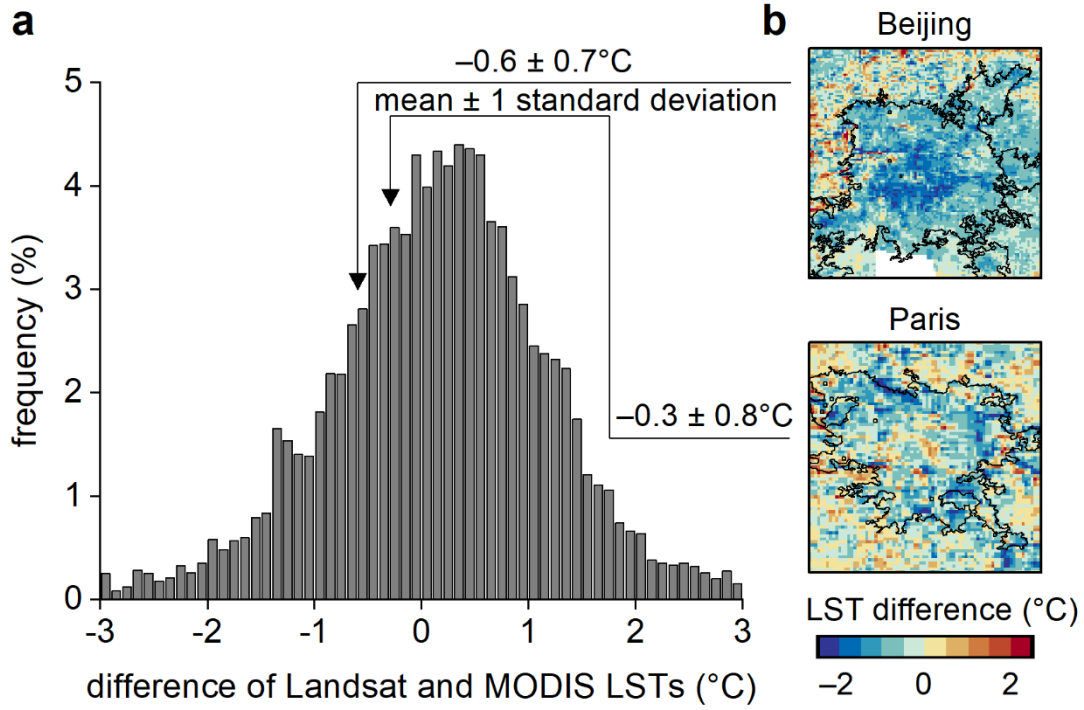

Figure S6. The spatial differences between the reconstructed Landsat land surface temperature (LST) and MODIS LST. The frequency distribution of LST difference over all pixels across global cities (**a**); and the spatial patterns of LST difference in Beijing, China and Paris, France (**b**).

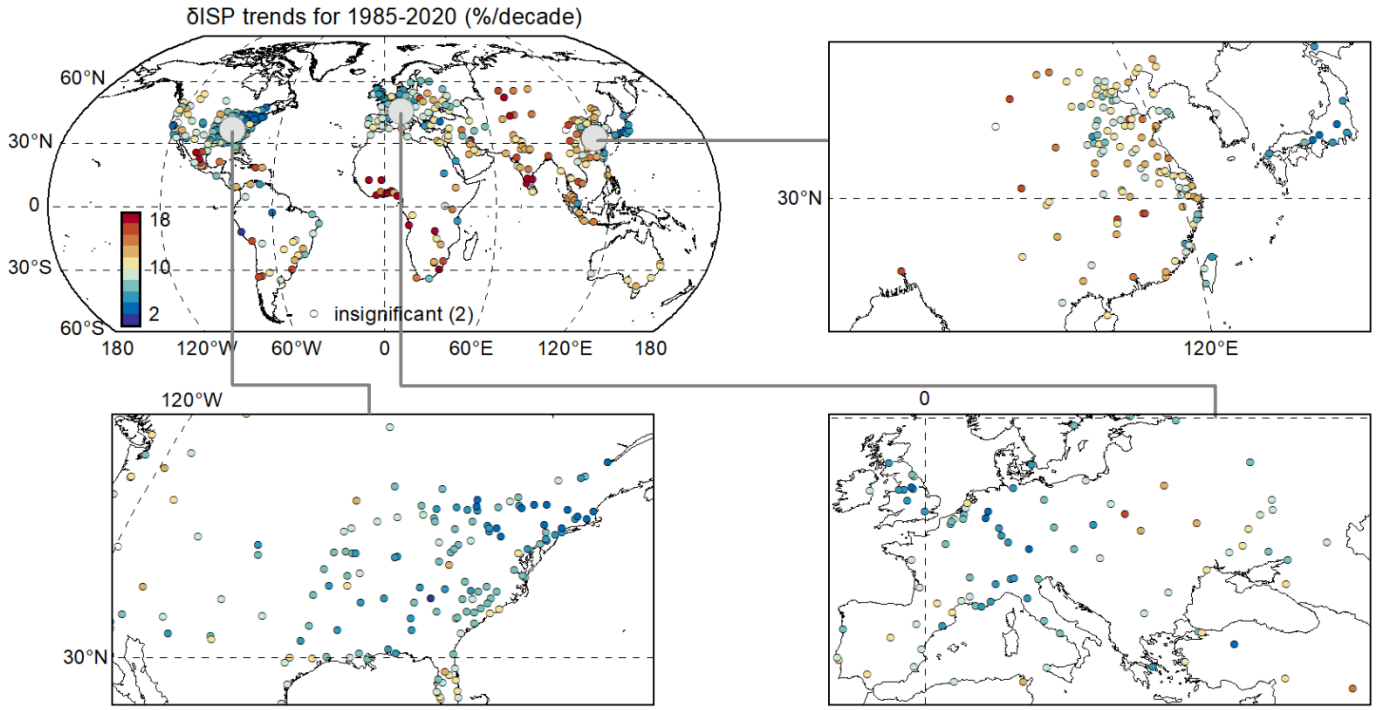

Figure S7. Urban-rural contrast in impervious surface percentage (δISP) trends since 1985 across global cities, with cities in the regions of North America, Europe, and Asia being enlarged further. The δISP trends were estimated from Landsat observations.

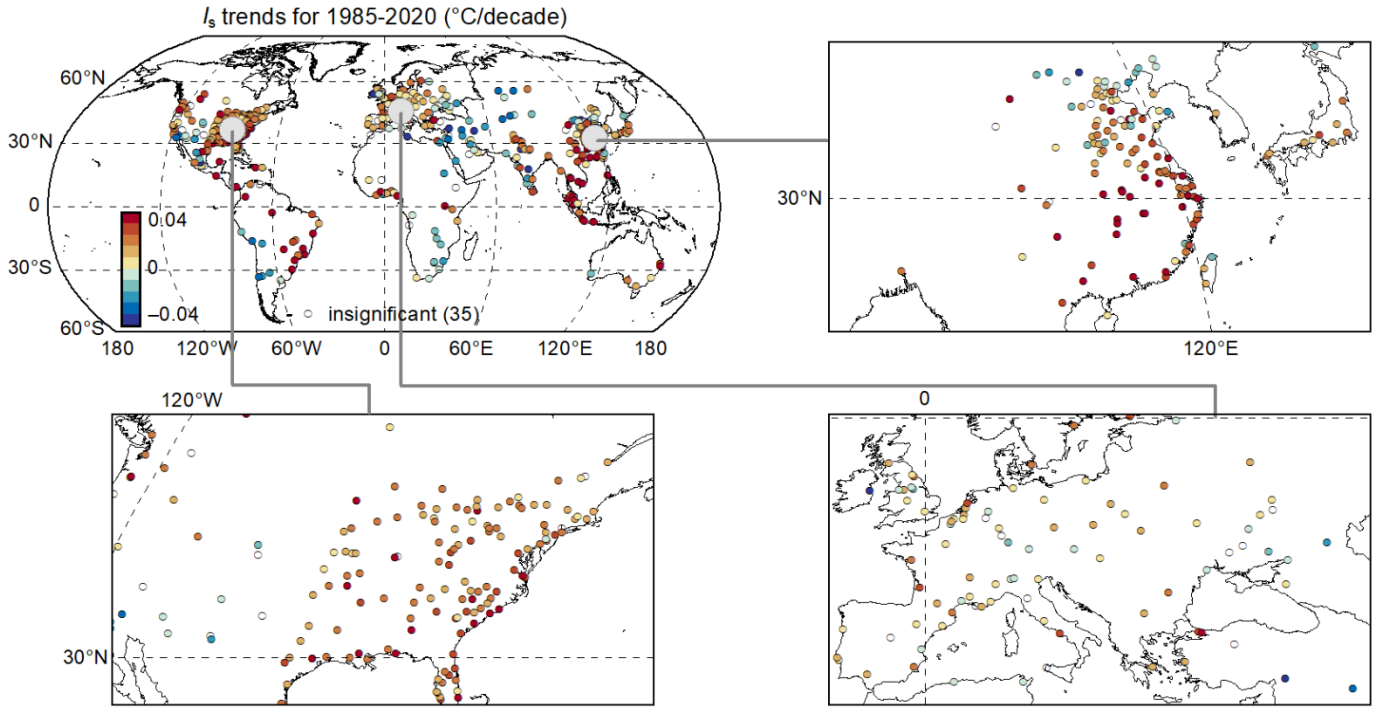

Figure S8. Surface urban heat island intensity (I_s) trends since 1985 across global cities, with cities in the regions of North America, Europe, and Asia being enlarged further. The I_s trends were estimated from Landsat observations.

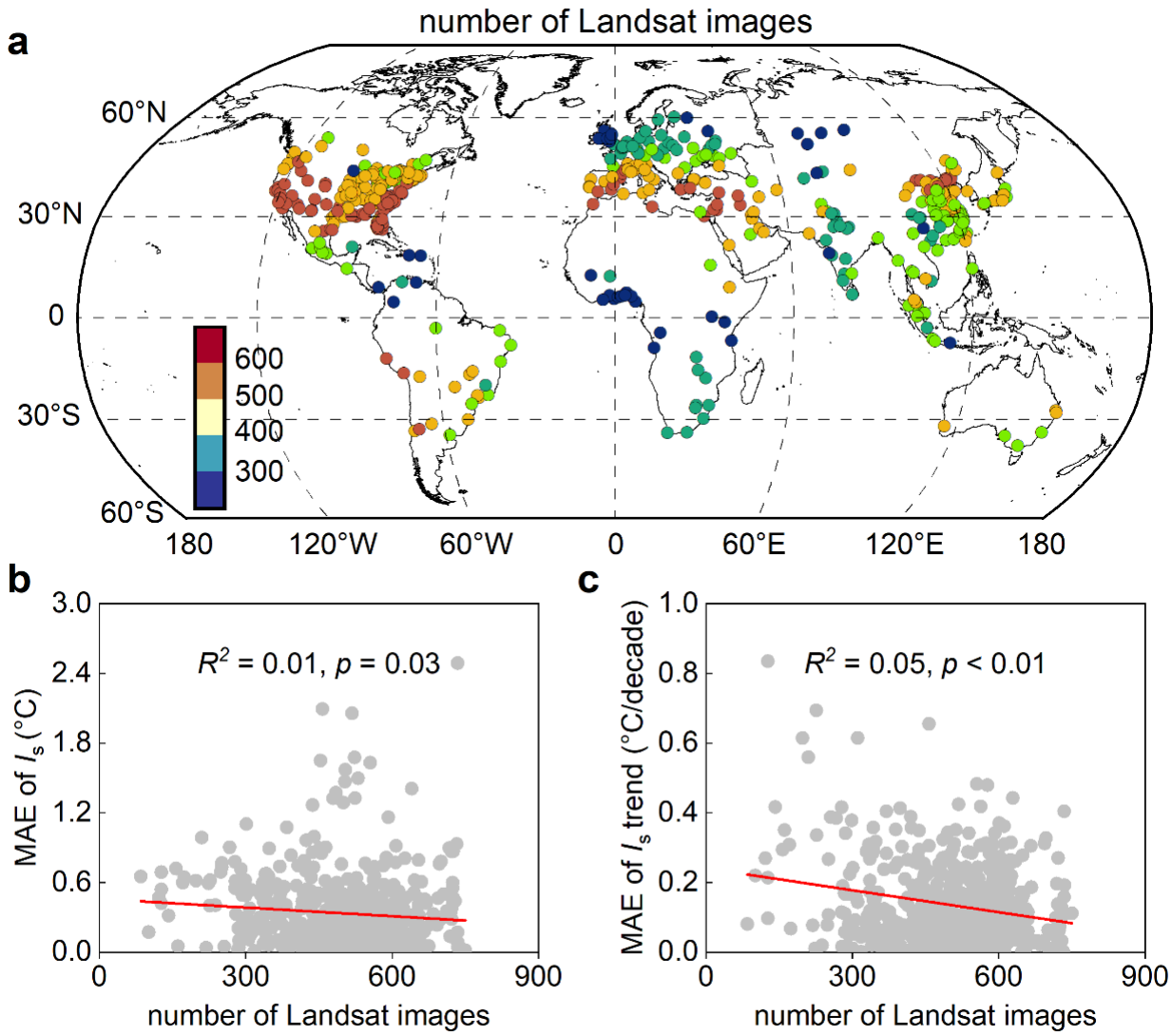

Figure S9. The impacts of disparities in the amount of available Landsat land surface temperature (LST) images on the mean absolute error (MAE) of surface urban heat island intensity (I_s) and I_s trends across global cities. Number of available Landsat LST imageries (**a**); relationships between the number of available Landsat LST imageries and MAE of I_s (**b**) and I_s trends (**c**) across global cities.

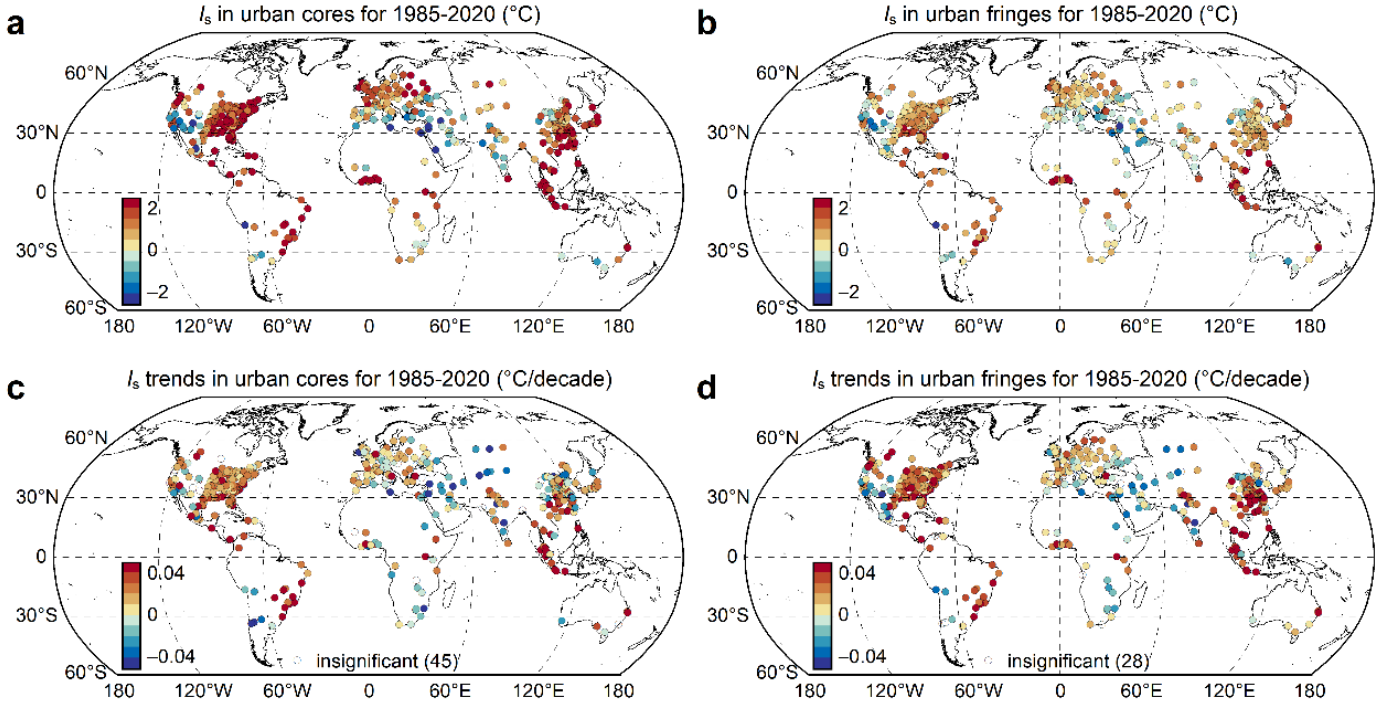

Figure S10. The surface urban heat island intensity (I_s) and I_s trend in different urban categories for 1985 – 2020. I_s in urban cores (**a**); I_s in urban fringes (**b**); I_s trend in urban cores (**c**); and I_s trend in urban fringes (**d**).

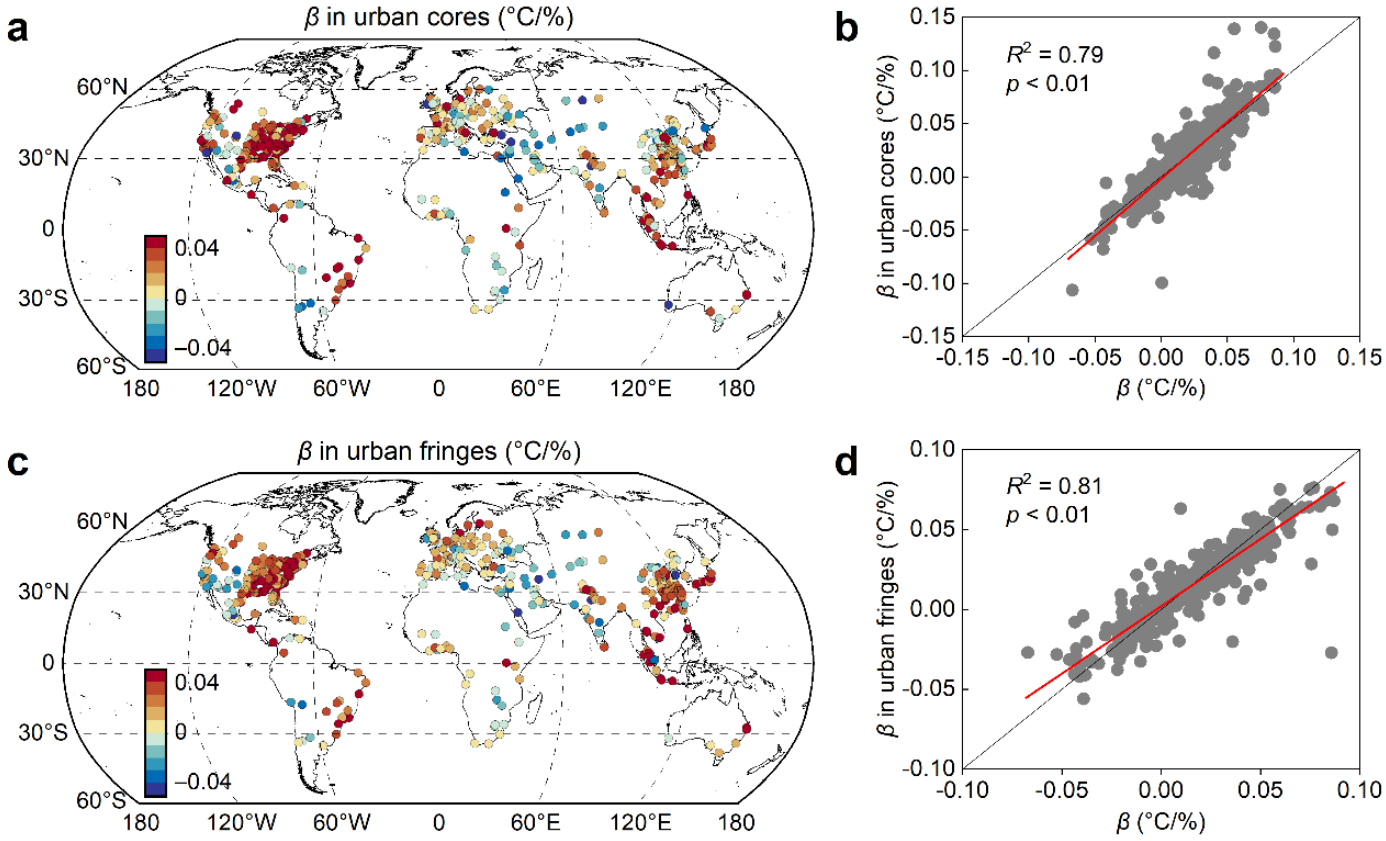

Figure S11. Spatial variations of urbanization-induced impacts on surface urban heat island intensity trends (β) in different urban categories. β in urban cores (**a**); correlation of β in urban cores with β (i.e., without distinguishing between urban categories) (**b**); β in urban fringes (**c**); and correlation of β in urban fringes with β (i.e., without distinguishing between urban categories) (**d**).

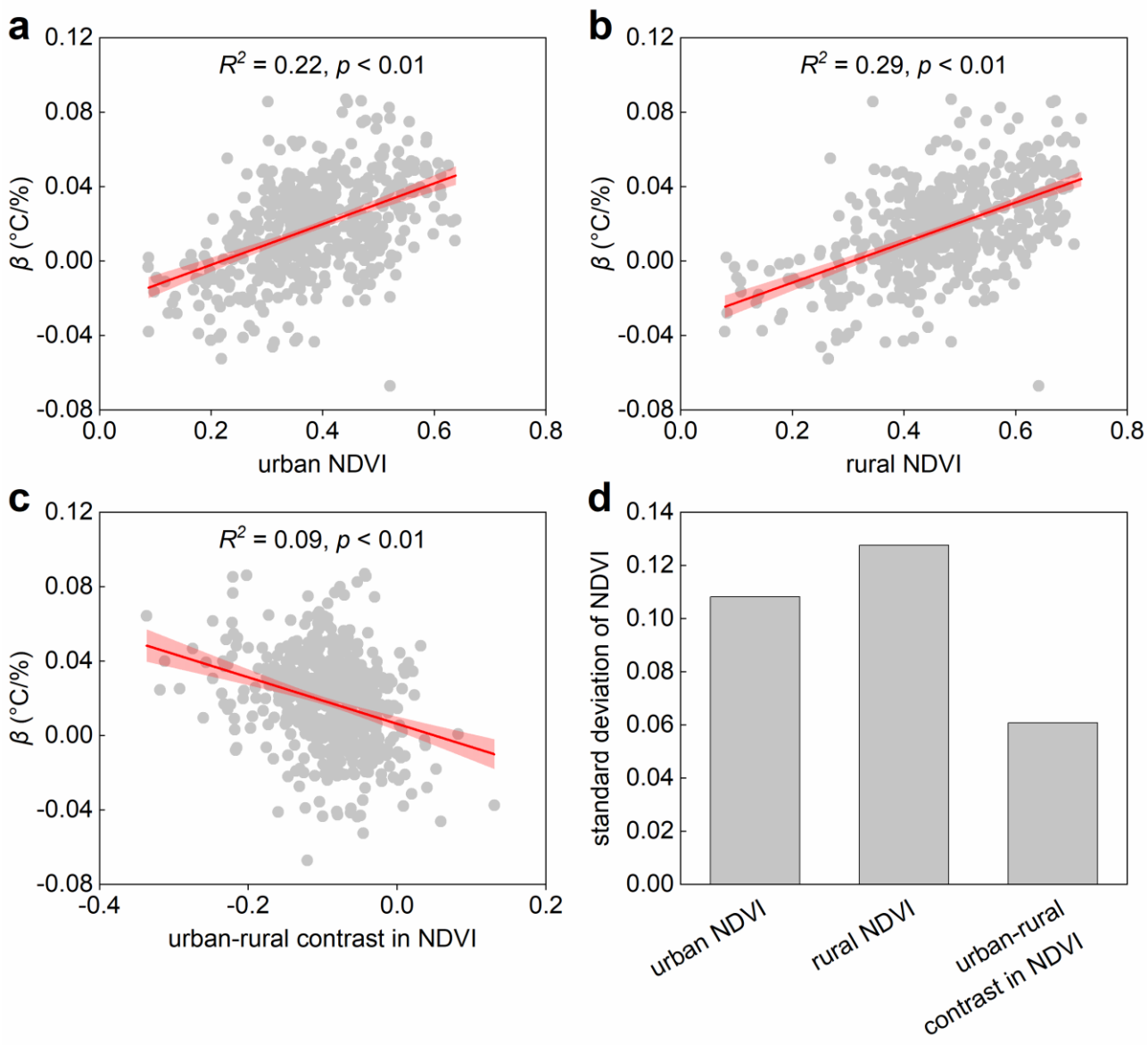

106

107 **Figure S12. Correlations of urbanization-induced impacts on surface urban heat island intensity**

108 **trends (*β*) with normalized difference vegetation index (NDVI).** Relationship of *β* with urban NDVI (**a**),

109 rural NDVI (**b**), and urban-rural contrast in NDVI (**c**); and standard deviation of three indicators (**d**).

110

111

112

B. Supplementary tables

Table S1. The ranking of the β (i.e., urbanization-induced impacts on surface urban heat island intensity trends) across countries. The mean and standard deviation (SD) of the β for each country.

List	Country	Abbreviation of country name	Mean	SD	Number of cities
1	Guatemala	GTM	0.0615	0	1
2	Malaysia	MYS	0.0605	0.0222	4
3	Indonesia	IDN	0.0558	0.0204	6
4	Philippines	PHL	0.0472	0	1
5	Panama	PAN	0.0471	0	1
6	Uganda	UGA	0.0470	0	1
7	Columbia	COL	0.0467	0	1
8	Vietnam	VNM	0.0444	0.0036	2
9	Denmark	DNK	0.0435	0	1
10	Thailand	THA	0.0401	0.0042	2
11	Brazil	BRA	0.0378	0.0129	13
12	Finland	FIN	0.0375	0	1
13	America	USA	0.0323	0.0233	145
14	Sri Lanka	LKA	0.0322	0	1
15	Sweden	SWE	0.0318	0	1
16	Japan	JPN	0.0281	0.0204	10
17	Tanzania	TZA	0.0268	0	1
18	Cambodia	KHM	0.0266	0	1
19	Netherlands	NLD	0.0265	0.0094	2
20	Canada	CAN	0.0255	0.0168	12

21	Dominica	DOM	0.0252	0	1
22	Australia	AUS	0.0212	0.0365	6
23	Romania	ROM	0.0211	0	1
24	Myanmar	MMR	0.0180	0	1
25	Bangladesh	BGD	0.0167	0	1
26	Nigeria	NGA	0.0163	0.0092	5
27	China	CHN	0.0163	0.0187	118
28	Belarus	BLR	0.0157	0	1
29	Pakistan	PAK	0.0154	0.0215	4
30	Bulgaria	BGR	0.0148	0	1
31	Belgium	BEL	0.0145	0.0050	3
32	Poland	POL	0.0139	0.0087	4
33	Ghana	GHA	0.0138	0.0244	2
34	Korea	KOR	0.0137	0	1
35	Portugal	PRT	0.0127	0.0078	3
36	Kenya	KEN	0.0125	0	1
37	France	FRA	0.0115	0.0140	13
38	Benin	BEN	0.0096	0	1
39	Cote d'Ivoire	CIV	0.0095	0	1
40	Puerto Rico	PRI	0.0089	0	1
41	Czech Republic	CZE	0.0070	0	1
42	Italy	ITA	0.0063	0.0164	8
43	Togo	TGO	0.0060	0	1
44	Great Britain	GBR	0.0059	0.0131	9
45	Hungary	HUN	0.0058	0	1
46	Spain	ESP	0.0055	0.0100	6

47	Greece	GRC	0.0041	0	1
48	Angola	AGO	0.0026	0	1
49	Egypt	EGY	0.0021	0.0203	2
50	India	IND	0.0021	0.0222	14
51	Qatar	QAT	0.0019	0	1
52	Morocco	MAR	0.0009	0	1
53	Mali	MLI	0.0007	0	1
54	Ethiopia	ETH	0.0001	0	1
55	Burkina Faso	BFA	-0.0005	0	1
56	Turkey	TUR	-0.0013	0.0382	5
57	Ukraine	UKR	-0.0019	0.0090	7
58	Kazakhstan	KAZ	-0.0024	0.0014	2
59	Germany	DEU	-0.0025	0.0112	8
60	South Africa	ZAF	-0.0028	0.0058	5
61	Russia	RUS	-0.0029	0.0141	11
62	Venezuela	VEN	-0.0030	0.0171	2
63	Tunisia	TUN	-0.0040	0	1
64	Mexico	MEX	-0.0049	0.0217	11
65	Syria	SYR	-0.0052	0	1
66	Congo	COD	-0.0070	0.0007	2
67	Algeria	DZA	-0.0085	0	1
68	Singapore	SGP	-0.0104	0	1
69	Zimbabwe	ZWE	-0.0105	0	1
70	Mozambique	MOZ	-0.0116	0	1
71	Austria	AUT	-0.0116	0	1
72	Chile	CHL	-0.0125	0	1

73	Azerbaijan	AZE	-0.0125	0	1
74	Kuwait	KWT	-0.0165	0	1
75	Saudi Arabia	SAU	-0.0166	0.0153	3
76	Argentina	ARG	-0.0178	0.0085	3
77	Iran	IRN	-0.0178	0.0212	2
78	Zambia	ZMB	-0.0179	0	1
79	Iraq	IRQ	-0.0181	0.0053	3
80	Israel	ISR	-0.0192	0	1
81	Kirghizia	KGZ	-0.0197	0	1
82	Uzbekistan	UZB	-0.0205	0	1
83	Bolivia	BOL	-0.0220	0	1
84	Peru	PER	-0.0245	0.0035	2
85	Turkmenistan	TKM	-0.0246	0	1
86	Sultan	SDN	-0.0282	0	1
87	Jordan	JOR	-0.0313	0	1
88	Libya	LBY	-0.0409	0	1
89	Ireland	IRL	-0.0671	0	1